Molecular Therapy
Methods & Clinical Development
Original Article

Amelioration of Muscle and Nerve Pathology in LAMA2 Muscular Dystrophy by AAV9-Mini-Agrin

Chunping Qiao,[1,5] Yi Dai,[2,5] Viktoriya D. Nikolova,[3,4] Quan Jin,[1] Jianbin Li,[1] Bin Xiao,[1] Juan Li,[1] Sheryl S. Moy,[3,4] and Xiao Xiao[1,4]

[1]Division of Pharmacoengineering and Molecular Pharmaceutics, UNC Eshelman School of Pharmacy, University of North Carolina at Chapel Hill, Chapel Hill, NC 27599, USA; [2]Department of Neurology, Peking Union Medical College Hospital, Chinese Academy of Medical Sciences, Beijing, Beijing, China 100730; [3]Department of Psychiatry, UNC School of Medicine, University of North Carolina at Chapel Hill, Chapel Hill, NC 27599, USA; [4]Carolina Institute for Developmental Disabilities, UNC School of Medicine, University of North Carolina at Chapel Hill, Chapel Hill, NC 27599

LAMA2-related muscular dystrophy (LAMA2 MD) is the most common and fatal form of early-onset congenital muscular dystrophies. Due to the large size of the laminin α2 cDNA and heterotrimeric structure of the protein, it is challenging to develop a gene-replacement therapy. Our group has developed a novel adeno-associated viral (AAV) vector carrying the mini-agrin, which is a non-homologous functional substitute for the mutated laminin α2. A significant therapeutic effect in skeletal muscle was observed in our previous study using AAV serotype 1 (AAV1). In this investigation, we examined AAV9 vector, which has more widespread transduction than AAV1, to determine if the therapeutic effects could be further improved. As expected, AAV9-mini-agrin treatment offered enhanced therapeutic effects over the previously used AAV1-mini-agrin in extending mouse lifespan and improvement of muscle pathology. Additionally, overexpression of mini-agrin in peripheral nerves of dy^w/dy^w mice partially amended nerve pathology as evidenced by improved motor function and sensorimotor processing, partial restoration of myelination, partial restoration of basement membrane via EM examination, as well as decreased regeneration of Schwann cells. In conclusion, our studies indicate that overexpression of mini-agrin into dy^w/dy^w mice offers profound therapeutic effects in both skeletal muscle and nervous system.

INTRODUCTION

Congenital muscular dystrophy (CMD) is a group of rare genetic muscle disorders that appear early in life from birth to 2 years of age. Characteristic signs include congenital hypotonia, delayed motor development, progressive muscle weakness, and dystrophic features visualized on muscle biopsy.[1,2] The most common form is muscular dystrophy type 1A (MDC1A, also named LAMA2-related muscular dystrophy, LAMA2 MD), which is responsible for 40% of all CMD cases. This subset is characterized by a primary deficiency in the laminin α2 chain of merosin (laminin-2, also termed Laminin211) caused by mutations within the *LAMA2* gene.[3,4] In general, complete laminin α2 deficiencies are functionally null mutations, leading to severe and non-ambulatory phenotypes; however, partial laminin α2 deficiencies tend to present with variable but comparatively milder phenotypes.[5]

The advent of next-generation sequencing technology has substantially improved CMD diagnosis, allowing for rapid and cost-effective CMD molecular testing in the clinic.[6] Consequently, the spectrum of LAMA2 MD has expanded in recent years partially due to the definitive diagnosis of molecular genetics.[7,8] Additionally, the International Standard of Care Committee for CMD recently published two consensus statements on standard of care and diagnostic approach for CMD to improve quality of life in CMD patients.[9,10] Evidence-based guidelines for CMD diagnosis and care were also released by the Review Panel of the American Association of Neuromuscular & Electrodiagnostic Medicine.[11,12]

The molecular pathogenesis of LAMA2 MD has not been fully elucidated, but several mechanisms have been proposed. Ervasti and Campbell[13] suggested that the laminin α2 chain confers a structural link from the extracellular matrix (ECM) to the cytoskeleton, stabilizing the muscle-cell membrane and imparting protection against contraction-induced damage. This hypothesis was challenged by Hall et al.[14] By using time-lapse photomicroscopy in a LAMA2 MD zebrafish model, they demonstrated that pathology of LAMA2 MD was through mechanically induced fiber detachment rather than sarcolemma rupture or fiber denervation.[14] Nevertheless, cell membranes are ruptured to some extent in mouse models with complete laminin α2 deficiency.[15]

Despite these recent advances in the diagnosis and understanding of LAMA2 MD, there is no approved treatment available for this debilitating disease.[16,17] The current clinical approach is centered on supportive care.[10,11] Over the past decade, various studies have been carried out on LAMA2 MD mouse models to test potential treatment options. Because the basement membrane is affected in LAMA2 MD, many of these approaches have targeted the expression of ECM

Received 19 December 2017; accepted 11 January 2018;
https://doi.org/10.1016/j.omtm.2018.01.005.

[5]These authors contributed equally to this work.

Correspondence: Xiao Xiao, PhD, Division of Pharmacoengineering and Molecular Pharmaceutics, Eshelman School of Pharmacy, University of North Carolina at Chapel Hill, Chapel Hill, NC 27599, USA.
E-mail: xxiao@email.unc.edu

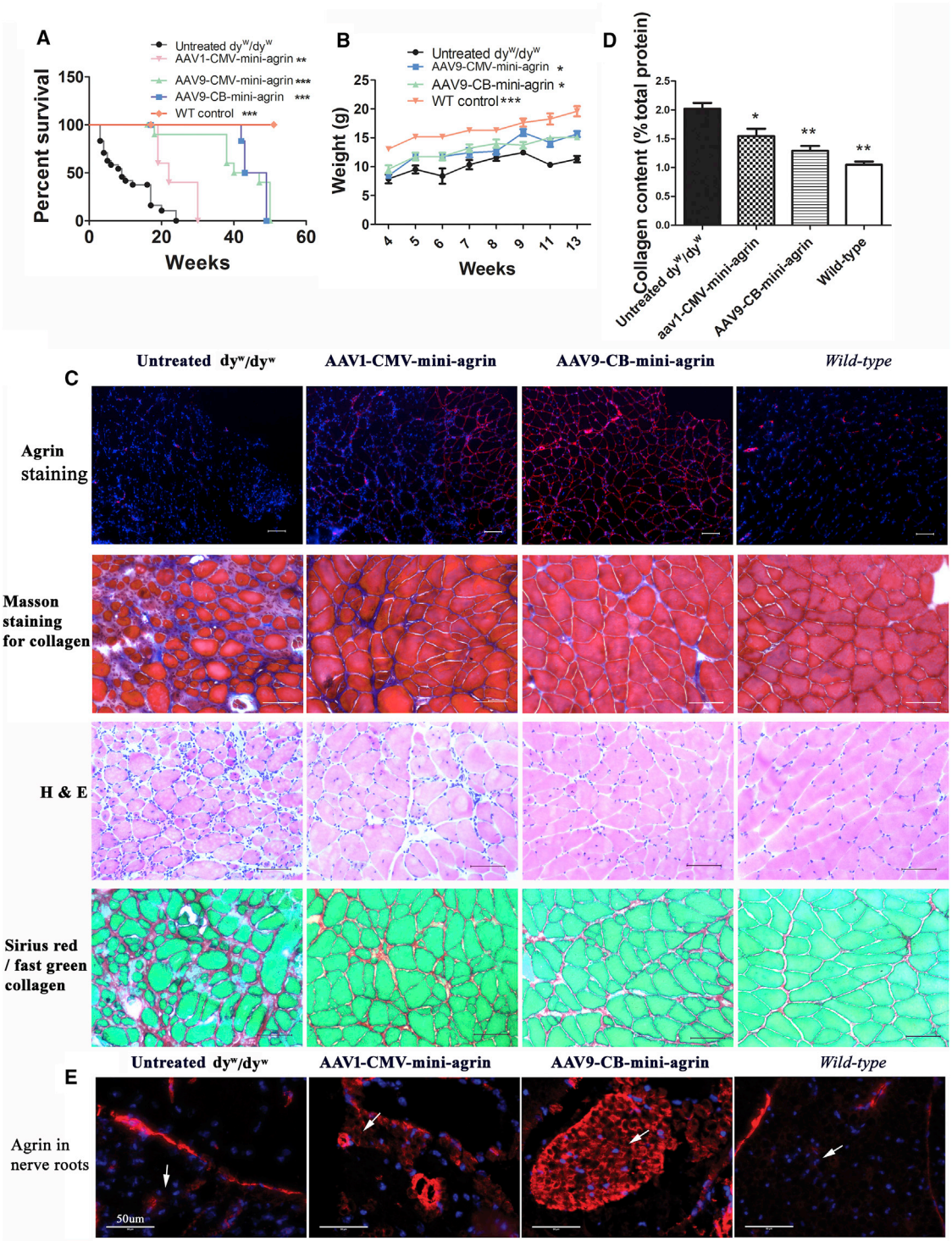

Figure 1. Lifespan, Growth Rate, and Pathology Improvement in the LAMA2 MD Mouse Model

(A) Lifespan of the treated mice was significantly extended. The vectors (2×10^{11} vg/pup) were delivered into homozygous dy^W/dy^W neonatal pups via intraperitoneal injection. n = 22 for untreated dy^W/dy^W group; n = 6 for AAV1-CMV-mini-agrin group; n = 9 for AAV9-CMV-mini-agrin group; n = 6 for AAV9-CB-mini-agrin group; n = 5 for wild-type (WT) control mice. **p < 0.01; ***p < 0.001. (B) Body weight of the treated mice was significantly increased. n = 7 for the untreated dy^W/dy^W and AAV9-CMV-mini-agrin mice; n = 6 for AAV9-CB-mini-agrin mice. *p < 0.05; ***p < 0.001. (C) Histology examination of triceps muscle. Mice were sacrificed at around 3 months of age. Agrin was stained

(legend continued on next page)

proteins. Transgenic expressions of the laminin α1, α2 chains, mini-agrin (a basement membrane-associated heparin sulfate proteoglycan), and other linker molecules in dy^w/dy^w mice, a model of LAMA2 MD, have been found to compensate for laminin-α2-chain deficiency.[4,18–22] Several approaches aimed to alleviate the secondary defects rather than to target the primary deficiency have been undertaken in LAMA2 MD. These approaches include inhibition of apoptosis,[23–26] interference with proteasomal and autophagy-mediated protein degradation,[27] as well as targeting fibrosis or inflammation in dystrophic muscle of LAMA2 MD mice.[28] It is worth mentioning that omigapil, an anti-apoptosis drug, is in phase I clinical trial with assessment of safety and tolerability for CMD (ClinicalTrials.gov Identifier: NCT01805024).[29]

Ideally, gene replacement therapy would offer curative treatment for LAMA2 MD patients. However, the size (>9 kb) of both laminin α1 and laminin α2 cDNA precludes their packaging into commonly used gene therapy vectors, such as adeno-associated viral (AAV) vectors. It is also unfeasible to generate a miniaturized laminin α chain, as it must incorporate into the laminin heterotrimer to be functional.[30] A potential solution to the packaging size limitation is the utilization of mini-agrin, a functional substitute gene. Mini-agrin shares with laminin α2 the ability to bind to α-dystroglycan, a protein that is involved in the linkage of basement membranes to the muscle sarcolemma.[30] Additionally, the immunological rejection of the protein will be minimal for clinical application because LAMA2 MD patients express agrin endogenously. Our group was the first to attempt somatic gene transfer of mini-agrin in mice.[31] Systemic delivery of mini-agrin into multiple vital muscles of LAMA2 MD mice using AAV vector significantly improved whole-body growth and motility and quadrupled the lifespan of the treated mice. One question from our previous study that remains unanswered is whether mini-agrin offers any beneficial effects to the nervous system and if so, to what extent.[31] In this study, we seek to investigate whether the therapeutic effects offered by AAV-mini-agrin could be further augmented by utilizing a more robust AAV serotype.

RESULTS

Improvement of Growth Rate and Lifespan after AAV9-Mini-Agrin Treatment

Previously, we utilized the AAV1 vector to deliver the mini-agrin gene because at that time AAV1 demonstrated superior transduction ability in skeletal muscle.[32] More recently, new AAV serotypes have been discovered, and AAV9 has demonstrated robust transduction of both skeletal muscle and nervous systems with greater efficiency than AAV1.[33,34] In this study, we performed a side-by-side comparison of these two serotypes to deliver mini-agrin gene. Additionally, we utilized a different ubiquitous promoter, CB (CMV enhancer and chicken β-actin promoter) versus the previously used CMV (cytomegalovirus) promoter to drive mini-agrin gene (Figure S6). The vectors (2×10^{11} vector genomes [vg]/mouse) were delivered into homozygous dy^w/dy^w neonatal pups (2 to 3 days of age) via intraperitoneal injection. The average lifespan of the untreated homozygous dy^w/dy^w mice was 10.18 ± 7.12 weeks (n = 22) (Figure 1A). Both AAV9-CMV-mini-agrin and AAV9-CB-mini-agrin treatments dramatically improved mouse lifespan (42.1 ± 10.6 weeks for CMV group, n = 9, $p < 0.001$ as compared to untreated control; 45.8 ± 3.4 weeks for CB group, n = 6, $p < 0.001$), and there was no significant difference in lifespan extension between AAV9-CMV-mini-agrin and AAV9-CB-mini-agrin groups (Figure 1A).

The average lifespan of the AAV1-CMV-mini-agrin-treated mice was 24 ± 5.6 weeks (n = 6), which was significantly shorter than that of the AAV9-CMV-mini-agrin group ($p < 0.001$) (Figure 1A). In addition, AAV9-CMV-mini-agrin and AAV9-CB-mini-agrin treatment significantly increased mouse body weight (Figure 1B). At 13 weeks, the average body weight of the untreated dy^w/dy^w mice was 11.31 ± 1.41 g (n = 7). The mean body weights of the AAV9-CMV-mini-agrin and AAV9-CB-mini-agrin-treated dy^w/dy^w mice were 15.65 ± 1.3 g (n = 7, $p < 0.01$) and 15.11 ± 1.03 g (n = 6, $p < 0.01$), respectively (Figure 1B). Taken together, our results indicate that AAV9-mini-agrin (driven by either CB or CMV promoter) improved therapeutic effects compared to AAV1-cmv-mini-agrin.

As expected, systemic delivery of both AAV9-mini-agrin and AAV1-cmv-mini-agrin in dy^w/dy^w mice resulted in overexpression of mini-agrin protein in body-wide muscle groups. Triceps (Figure 1) and diaphragm muscles (Figure S1) are presented as examples here. The wild-type agrin is expressed in the neuromuscular junction (appearing as punctuated staining) and blood vessel wall in the wild-type and untreated dy^w/dy^w mice. The treatment led to overexpression of mini-agrin in the ECM of the skeletal muscles as revealed via immunofluorescent staining, with more uniform distribution in the AAV9 group than the AAV1 group (Figure 1C). We additionally examined muscular dystrophic pathology amendment by the treatment through H&E staining for general morphology, Masson's trichrome stain, and Sirius red stain for collagen deposition. As compared to the wild-type muscle, the dystrophic muscle displayed varied muscle fiber sizes and mononuclear cell infiltration on H&E staining. It also showed increased collagen accumulation in ECM of the skeletal muscles on both Masson's trichrome stain and Sirius red/fast green stain (Figures 1C and S1). Overexpression of mini-agrin in both groups led to more uniform muscle fiber sizes, reduced mononuclear cell infiltration, and decreased collagen deposition (Figures 1C, S1, S5, and S7). Collagen quantification data further confirmed decrease of the collagen accumulation in the treated muscle. The collagen content of wild-type triceps muscle was 1.04% ± 0.12% ($p < 0.001$ as compared to untreated homo), and the collagen content of the untreated dy^w/dy^w triceps

red, and nuclei were stained with DAPI as shown in blue. (D) Quantification of collagen content in the triceps muscle shown in (C) of Sirius red/fast green staining. n = 7 for the untreated dy^w/dy^w; n = 6 for AAV9-CB-mini-agrin group; n = 3 for AAV1-CMV-mini-agrin group; n = 5 for wild-type mice. One-way ANOVA plus Dunnett posteriori test was used as statistical method. For the posteriori test, all groups were compared with the untreated dy^w/dy^w mice. *$p < 0.05$; **$p < 0.01$. (E) Mini-agrin expression in nerve roots. White arrow pointed to the nerve root area. Agrin was stained red, and nuclei were stained blue. Scale bar, 50 μm. Error bar indicates SEM.

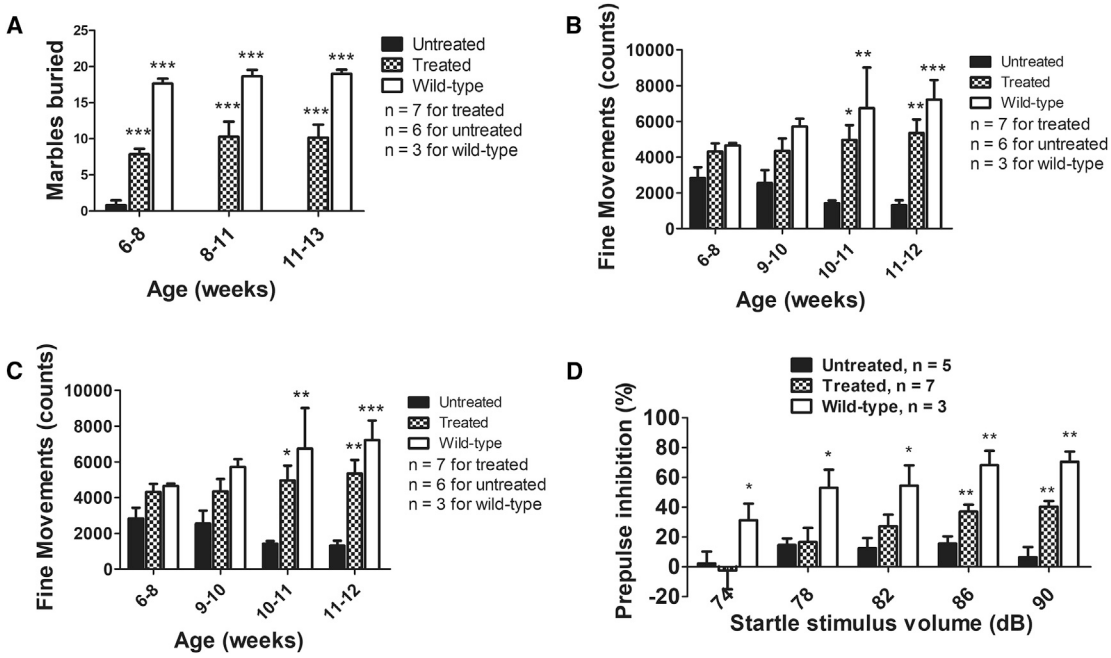

Figure 2. Improvement of Motor Function and Sensory Processing by Treatment in the LAMA2 MD Mouse Model

The AAV9-CB-mini-agrin vector was delivered into dy^w/dy^w neonatal pups (2×10^{11} vg/pup) via temporal vein injection. (A) Marble-burying test revealed that the treated mice buried significantly more marbles. (B) Fine movements (repeated breaking of horizontal photobeams) during an open-field test. (C) Rearing movements during an open-field test. (D) Prepulse inhibition (PPI) of the acoustic startle response. dB, decibels. Two-way ANOVA plus Bonferroni posttest using Graph Pad Prism software were applied. *$p < 0.05$; **$p < 0.01$; ***$p < 0.001$ as compared to the untreated age-matched controls. Error bar indicates SEM.

muscle was 2.01% ± 0.27% (Figure 1D). The collagen content of the two treated groups, AAV1-mini-agrin and AAV9-mini-agrin, was 1.5% ± 0.21% ($p < 0.05$) and 1.29% ± 0.205 ($p < 0.001$), respectively (Figure 1D). This clearly indicates muscle pathology improvement by overexpression of mini-agrin.

Improvement of Motor Function and Sensorimotor Processing in the LAMA2 MD Mouse Model

To evaluate whether AAV9-mini-agrin treatment results in any behavioral improvement in dy^w/dy^w mice, the marble-burying and open-field tests were used. For this study, the AAV9-CB-mini-agrin vector was delivered into neonatal homozygous dy^w/dy^w pups via temporal vein injection (2×10^{11}vg/pup). The marble-burying test takes advantage of the proclivity of mice to dig in natural settings, while the open-field test assesses both horizontal and vertical (i.e., rearing) activity levels.[35] As shown in Figure 2A, untreated dy^w/dy^w mice could barely bury any marbles (0.83 ± 1.6) even at a young age (6 to 8 weeks of age). The AAV9-mini-agrin-treated mice could bury as many as 16 marbles (10.16 ± 4.40) at 13 weeks of age (two-way ANOVA, $p < 0.0001$). Exploratory motor activity in a novel environment of the mice was assessed by an open-field test. The untreated dy^w/dy^w mice were hypoactive, as revealed by progressive decline in fine movements (an index of horizontal movements; Figure 2B) and rearing movements (Figure 2C). In contrast, the treated dy^w/dy^w mice maintained normal levels of fine movements until the end of the experiments (n = 3–7, two-way ANOVA, $p < 0.0001$). Vertical rearing movements by the treated mice were significantly improved at earlier ages (6 to 8 weeks of age); however, the activity decreased with age (Figure 2C). We also examined mini-agrin expression in brain and spine, including the nerve roots. There was no difference of agrin expression in the brain and spinal cord between treated and control mice; however, there was remarkable and even transgene expression in the AAV9-mini-agrin-treated nerve roots (Figure 1E). Patchy mini-agrin expression was observed in the AAV1-mini-agrin treated nerve roots as compared with the untreated group. This indicated that the treatment delayed the hind leg paralysis of the mice but could not cure it. General behavioral improvement of the treated mice is also demonstrated in video recordings (Figures S2 and S3).

Additionally, we measured the acoustic startle responses, which can provide general information regarding sensorimotor processing. Measurement of the reflex under conditions that engage the influence of higher brain centers can predict forebrain function. In the case of acoustic startle responses, presentation of lower intensity acoustic stimuli immediately prior to the acoustic startle stimulus decreases the response to the startle stimulus. This phenomenon, called prepulse inhibition (PPI) of startle reflex, is regulated by forebrain neural circuits and is considered an operational measure of sensorimotor gating, a filtering mechanism to modulate information flow in the brain, allowing selective allocation of attentional resources to salient stimuli.[35] Deficits in PPI are an indicator of deficiencies in the cognitive processes underlying this sensorimotor gating.

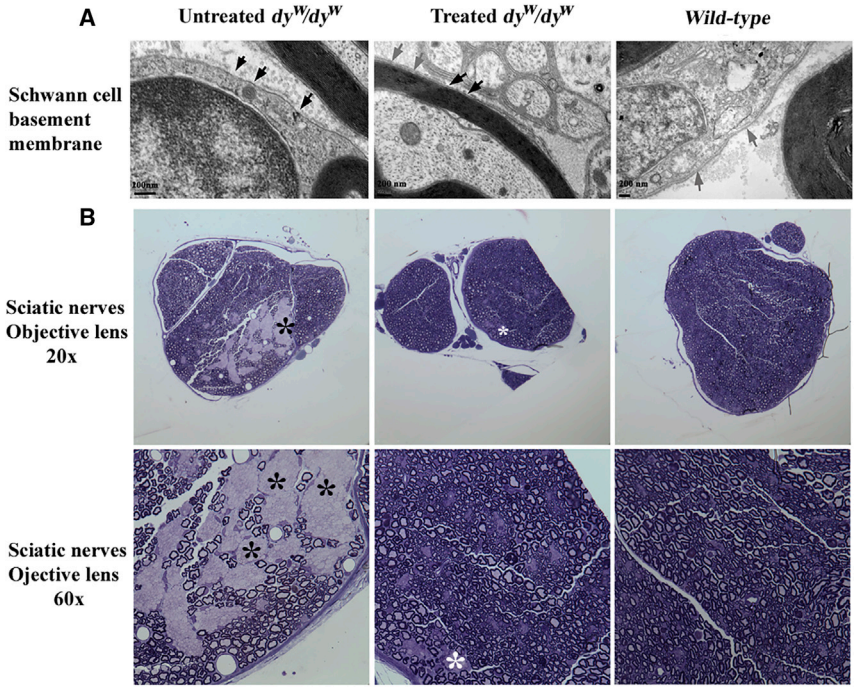

Figure 3. Amelioration of Peripheral Neuropathy

n = 2 for the untreated dy^w/dy^w mice and wild-type mice, and n = 3 for the AAV9-CB-mini-agrin-treated mice. (A) Partial restoration of Schwann cell basement membrane examined by transmission electron microscopy (TEM). Black arrowheads point to patchy or discontinuous basement membrane; gray arrowheads show dense and continuous shades. (B) Myelination of nerve axon was notably improved via toluidine blue staining under light microscopy. Black star indicates segregation of a large area of unmyelinated nerve fibers in the untreated mice; white star indicates small areas of unmyelinated nerve fibers in the treated counterparts.

In the present study, the untreated dy^w/dy^w mice had overt decreases in PPI, in comparison to the wild-type mice, across all prepulse sound levels (Figure 2D). However, the AAV9-mini-agrin-treated mice showed significantly enhanced PPI at the higher prepulse levels: 86 dB (15.6 ± 9.5 in untreated versus 40.4 ± 12.7 in treated versus 68.1 ± 16.9 in the wild-type mice) and 90 dB (9.6 ± 15.7 in untreated versus 39.2 ± 10.4 in treated versus 70.5 ± 11.7 in the wild-type mice) (Figure 2D). This clearly demonstrates the AAV-mini-agrin treatment led to partial rescue of impaired sensorimotor processing in the LAMA2 MD model.

Partial Restoration of Schwann Cell Basement Membrane and Improvement of Regeneration of Schwann Cells

Since we had observed much delayed hind-leg paralysis in the treated mice, we next sought to investigate whether the congenital hypomyelination had been amended. At 4 months of age, the control (n = 2) and treated mice (n = 3) were sacrificed, and their sciatic nerves were examined by transmission electron microscopy (TEM). Laminin α2 is a major component in both skeletal muscle and Schwann cells. In the present study, laminin α2 deficiency in dy^w/dy^w mice resulted in patchy or discontinuous basement membrane of Schwann cells in sciatic nerves (Figure 3A, black arrowhead) under TEM examination. The wild-type basement membrane displayed dense and continuous staining (Figure 3A, gray arrow). As expected, the phenotype of Schwann cells basement membranes was vastly improved by treatment; we observed a continuous membrane in most parts with occasional patchy spots (Figure 3A).

To further examine the amelioration of nerve pathology, we also employed light microscopy to investigate the myelinated nerve fibers with the gold standard method of toluidine blue staining.[36] As displayed in Figure 3B, the sciatic nerves of untreated dy^w/dy^w mice showed segregation of a large area of unmyelinated nerve fibers (black star), while the nerves from wild-type mice exhibited evenly distributed unmyelinated and myelinated axons. The nerve fibers from the treated dy^w/dy^w mice displayed relatively even distribution between myelinated and unmyelinated nerve fibers with occasional segregation of small area(s) of unmyelinated nerve fibers (white star). This clearly indicated improvement of myelination of the treated nerve fibers.

Laminin α2 appears to have both a structural role in formation of the Schwann cell basal lamina and a signaling role through dystroglycan and integrin receptors.[37] Here, we intended to study how overexpression of mini-agrin affected Schwann cell development in the sciatic nerve of the laminin α2-deficient mice. Immunofluorescent staining against a myelinating Schwann cell proliferation marker (Oct6, a critical transcriptional factor for Schwann cell proliferation) on sciatic nerve cryo-sections was performed.[38] As shown in Figure 4A, there were no Oct6-positive cells in the sciatic nerves of normal wild-type mice. Unlike wild-type mice, there were significant amounts of Oct6-positive cells (31 ± 8.08^+ cells/ CSA [cross-sectional area]) in the untreated dy^w/dy^w sciatic nerves, indicating regeneration of Schwann cells. In the treated sciatic nerves, the Oct6-positive cells were significantly reduced (13.5 ± 3.10 cells/CSA, n = 4, $p < 0.001$) (Figure 4B). This demonstrated improvement of regeneration of Schwann cells by overexpression of mini-agrin in peripheral nervous system in dy^w/dy^w mice.

DISCUSSION

Among different subtypes of CMDs, LAMA2 MD is the most common subtype and accounts for approximately 40% of all cases. Currently, there are no effective treatment options for any of the CMDs. Because of the large size of the laminin α2 cDNA and the heterotrimeric feature of the laminin α2 protein, it is particularly challenging to develop gene replacement therapy for LAMA2 MD. In our previous study, systemic delivery of an alternative functional gene, mini-agrin, utilizing AAV1 vector had a profound therapeutic

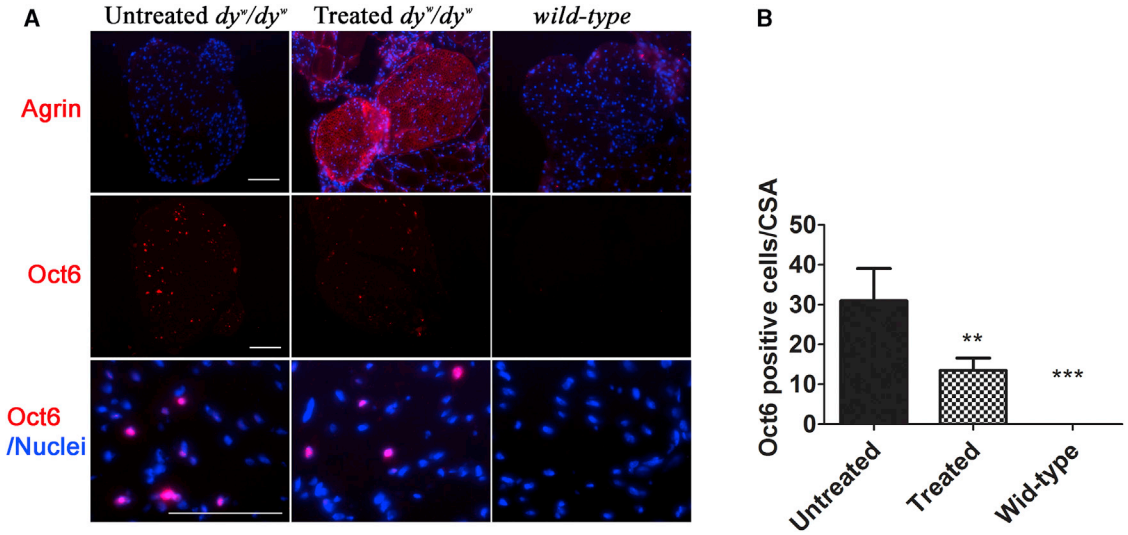

Figure 4. Reduction of Schwann Cell Regeneration by the Treatment

The treated mice were delivered with AAV9-CB-mini-agrin at neonatal age. (A) Immunofluorescent staining against pro-myelinating Schwann cell marker Oct6. Nuclei were stained blue with DAPI. (B) Quantification of Oct6-positive cells. All positive cells were counted, and at least three mice were utilized for each group. **$p < 0.01$; ***$p < 0.001$. Error bar indicates SEM.

effects in skeletal muscle.[31] In this manuscript, we extended our previous investigation by using the more robust AAV9 serotype to examine whether therapeutic effects could be further improved. Additionally, we investigated whether nerve pathology could also be ameliorated by overexpression of mini-agrin.

We now report several key discoveries in our study. First, AAV9 vector offers superior therapeutic effects compared to the AAV1 serotype in dy^w/dy^w mice. Second, treatment not only ameliorates muscle pathology, but also improves peripheral neuropathy and cognitive processing. Third, we show that phenotyping approaches, such as the marble-burying assay, open-field test, and acoustic-startle procedure, may be used to systematically evaluate motor dysfunction and sensorimotor gating deficits in the dy^w/dy^w mice. Unlike other dystrophic animal models, which only exhibit mild debilitation, the phenotype of dy^w/dy^w mice is severe. Untreated dy^w/dy^w mice rarely survive past 3 months of age. Due to the severity of the dy^w/dy^w phenotype, traditional motor functional tests such as treadmill running are not suitable. On the other hand, the approaches described in this investigation provide objective methods for muscle and nerve functional evaluation for CMD research that are both feasible and reliable.

Indeed, our data indicated that AAV9-mini-agrin treatment resulted in motor functional improvements in a marble-burying assay and delayed hind leg impairment in an open-field test, as well as improved sensory processing in brain, demonstrated via the acoustic-startle assay. Furthermore, electron microscopic examination revealed partial restoration of basement membrane of Schwann cells in peripheral nerves of the treated mice. Light microscopy revealed less segregation of unmyelinated nerve fibers as compared to the untreated counterpart. Immunofluorescent staining against a pro-myelinating Schwann cell marker (Oct6) indicated improvement of regeneration of Schwann cells in the treated peripheral nerves. All together, this study indicates that systemic delivery of AAV9-mini-agrin vector into dy^w/dy^w mice offers therapeutic effects in both skeletal muscle and nervous systems.

Interestingly, overexpression of mini-agrin in dy^w/dy^w mice was able to facilitate their fertility, suggesting widespread therapeutic benefits, since the homozygous dy^w/dy^w mice are not fertile. We did obtain one homozygous dy^w/dy^w pregnant female after treatment with AAV9-mini-agrin vector (Figure S4). Genotyping showed that all pups were homozygous dy^w/dy^w, indicating both treated male and female parental dy^w/dy^w mice were fertile. Although we only obtained one pregnant female, this data indicates mini-agrin can partially compensate for the function of laminin α2 in reproductive organs as well as overall health. Consistently, it was reported that overexpression of laminin α1 chain in testis by transgenic technology significantly reversed the histopathologic feature of the testis in laminin α2-deficient dy^{3k}/dy^{3k} mice.[39] However, only pathological studies were described, and no actual fertility experiments were performed.[39]

It is important to note that overexpression of mini-agrin in peripheral nerves of dy^w/dy^w mice only delayed hindlimb paralysis, and it is not a cure. Most of the AAV9-mini-agrin-treated dy^w/dy^w mice still developed progressive paralysis 3 months after treatment, although they were free to move around by crawling with forelimbs. In fact, the progressive lameness of hindlimbs also appeared in both laminin α2 and mini-agrin transgenic dy^w/dy^w mice.[4,18] In this study, we purposely utilized the ubiquitous CMV or CB promoter to achieve transgene expression in peripheral nerves. However, in the clinic, neuropathology damage in most of the CMD patients may not be reversible.[40]

Muscle-specific promoters, which could reduce non-specific expression in undesired organs such as the liver, could be considered for future clinical applications.[41] Infants with CMD often have severe weakness, decreased muscle tone, floppiness, and congenital contractures[1]. Whereas peripheral neuropathy is a prominent feature in all mouse models of LAMA2 CMD, the muscular dystrophic pathology is the predominant phenotype observed in human patients.[9,22,42] In this regard, the AAV-mini-agrin has been shown here to significantly improve muscle strength and partially alleviate nerve pathology in mice. It is therefore a promising candidate in the search for LAMA2-related CMD clinical treatments.

A previous study indicated that Schwann cell maturation and myelination of motor axons were partially inhibited in the absence of laminin α2, whereas, perhaps as a compensatory mechanism, there was an increase in proliferation and a subsequent accumulation of Schwann cells at earlier pre- and/or pro-myelinating stage of differentiation.[43] Similarly, we also observed (a) dramatic increase(s) of pro-myelinating Schwann cell marker Oct6 in the peripheral nerves of dy^w/dy^w mice. Most importantly, our results showed that overexpression of mini-agrin significantly decreased $Oct6^+$ cells in peripheral nerves. This phenomenon is in line with the nerve pathology alleviation as evidenced by toluidine blue staining as well as motor activity improvement. Our results indicate that Oct6 expression could be used as an index to measure therapeutic efficacy in peripheral nerves for LAMA2-related CMD preclinical application. It is noteworthy that amelioration of peripheral neuropathy has also been previously reported in dy^{3k}/dy^{3k} mice by overexpressed laminin α1 gene via transgenic technology.[44] The presence of laminin α1 chain in the peripheral nervous system resulted in near normal myelination, restored Schwann cell basement membranes, and improved rotarod performance.[44] However, similar to the difficulty of using laminin α2, the gene of laminin α1 is too big to be delivered by most of the viral vectors for therapeutic applications.

It appears that agrin possesses other functions in addition to serving as a linker molecule substituting the laminin α2. One most recent report shows that a single administration of agrin protein promoted cardiac regeneration in adult mice after myocardial infarction.[45] The report also implied that agrin treatment had other beneficial effects in addition to promoting cardiomyocyte regeneration, such as inhibition of fibrosis, modulation of the immune response, and angiogenesis.[45] It will be very interesting to see if mini-agrin would offer similar therapeutic effects as agrin does in this context in our future work.

In conclusion, our study indicates that delivery of AAV-mini-agrin vector offers therapeutic effects in both skeletal muscle and peripheral nerves, representing one of the most promising therapeutic approaches for LAMA2 related CMD. In the future, we will evaluate and optimize human-mini-agrin construction, by applying muscle-specific promoters and possibly performing combination therapy of mini-agrin together with other linker molecules to further improve its therapeutic potential.[21,22]

MATERIALS AND METHODS

Plasmid Construction and AAV Vector Production

The original mouse mini-agrin cDNA was generated by a RT-PCR method from mouse kidney tissue as described previously.[31] The mini-agrin cDNA was then cloned into AAV vector plasmid under the transcriptional control of CB promoter (chicken β-actin promoter and CMV enhancer),[46] and the final construct was named pXX-CB-mini-agrin. AAV serotype 9 was chosen as our delivery vehicle to achieve robust transgene expression in both skeletal muscle and peripheral nervous system,[46] and the final vector was named AAV9-CB-mini-agrin. The AAV vector was produced by a triple transfection method, and the virus was purified by polyethylene glycol (PEG) precipitation followed by CsCl ultracentrifugation.[47] The titer of AAV vector was determined by both dot-blot and RT-PCR methods. The concentration of viral vector stock was in the range of 2×10^{12} to 1×10^{13} vg/mL.

Mice and Vector Administration

All experiments involving animals were approved by the University of North Carolina Institutional Animal Care and Use Committee (IACUC). The heterozygous breeding pairs of dy^w/dy^w mice (Stock no. 013786/dy^w) were purchased from The Jackson Laboratory (Bar Harbor, ME). The pregnant females and neonatal pups were bred at UNC animal facilities. The AAV1-CMV-mini-agrin and the AAV9-CMV-mini-agrin vectors were delivered into neonatal dy^w/dy^w mice via intraperitoneal injection (100 μL of 2 to 5×10^{12} vg/mL). The AAV9-CB-mini-agrin vector was delivered into the neonates (2 to 3 days age) of dy^w/dy^w mice by temporal vein injection with 80 μL of the vector (2 to 5×10^{12} vg/mL) per mouse.

Marble-Burying Assay for Digging Ability

Mice were tested in a Plexiglas cage located in a sound-attenuating chamber with ceiling light and fan.[35] The cage contained 5 cm of corncob bedding, with 20 black glass marbles (14 mm diameter) arranged in an equidistant 5 × 4 grid on top of the bedding. Subjects were given access to the marbles for 30 min. Measures were taken of the number of buried marbles (two-thirds of the marble covered by the bedding).

Open-Field Test for Activity and Motor Function

Mice were assessed by 60-min trials in an open-field chamber (41 cm × 41 cm × 30 cm), crossed by a grid of photobeams (VersaMax system, AccuScan Instruments).[35] Counts were taken of the number of photobeams broken during the trial, with separate measures for horizontal activity (repeated breaking of photobeams) and rearing movements.

Acoustic-Startle Procedure for Sensorimotor Gating

The acoustic startle measure was based on the reflexive whole-body flinch, or startle response, following exposure to a sudden noise. Animals were tested with a San Diego Instruments SR-Lab system, using published methods.[35] In brief, mice were placed in a small Plexiglas cylinder within a larger, sound-attenuating chamber (San Diego

Instruments). The cylinder was seated upon a piezoelectric transducer, which allowed vibrations to be quantified and displayed on a computer. The chamber included a ceiling light, fan, and a loudspeaker for the acoustic stimuli (bursts of white noise). Background sound levels (70 dB) and calibration of the acoustic stimuli were confirmed with a digital sound level meter (San Diego Instruments). Each test session consisted of 42 trials, presented following a 5-min habituation period. There were seven different types of trials: the no-stimulus trials, trials with the acoustic startle stimulus (40 ms; 120 dB) alone, and trials in which a prepulse stimulus (20 ms; either 74, 78, 82, 86, or 90 dB) had onset 100 ms before the onset of the startle stimulus. The different trial types were presented in blocks of seven, in randomized order within each block, with an average intertrial interval of 15 s (range, 10–20 s). Measures were taken of the startle amplitude for each trial, defined as the peak response during a 65-ms sampling window that began with the onset of the startle stimulus. Levels of PPI at each prepulse sound level were calculated as 100 − ([response amplitude for prepulse stimulus and startle stimulus together/response amplitude for startle stimulus alone] × 100).

TEM Method

Mice were perfused with a fixative containing 2% paraformaldehyde and 2.5% glutaraldehyde in 0.15 M sodium phosphate buffer (pH 7.4). After perfusion, sciatic nerves were dissected and stored for several days in the fixative before processing for electron microscopy. Following three rinses with 0.15 M sodium phosphate buffer, the samples were post-fixed for 1 hr in 1% osmium tetroxide in sodium phosphate buffer. The nerves were dehydrated through increasing concentrations of ethanol (30%, 50%, 75%, 100%, 100%, 10 min each) and two changes of propylene oxide (15 min each). Samples were infiltrated in a 1:1 mixture of propylene oxide: Spurr's epoxy resin (Polysciences, Warrington, PA) overnight followed by 24 hr in 100% resin. The nerves were embedded in fresh epoxy resin and polymerized overnight at 70°C. Seventy-nanometer ultrathin sections of selected nerves were cut, mounted on 200 mesh copper grids, and post-stained with 4% aqueous uranyl acetate for 15 min, followed by Reynolds' lead citrate for 7 min.[48] Sections were observed using a LEO EM910 transmission electron microscope operating at 80 kV (Carl Zeiss SMT, Peabody, MA) and photographed using a Gatan Orius SC1000 Digital Camera and Digital Micrograph 3.11.0 (Gatan, Pleasanton, CA).

Toluidine Blue Staining of Sciatic Nerves

For light microscopy, 1 μm cross thin-sections of the nerves were cut using a diamond knife, mounted on glass slides, and stained with 1% toluidine blue O in 1% sodium borate. Sections were heated on a drop of water on a 55°C–60°C hotplate until the sections were flat and well adhered to the slide—about 2–3 minutes. The slide was left on the hotplate, and the sections were covered with several drops of stain. The stain remained on the slide until a metallic-looking rim formed around the edge of the stain droplet, and then the slide was rinsed gently with deionized water. The stained sections were mounted with an acrylic mounting medium, such as Polymount (Polysciences) or DPX (Fluka). The staining was photographed using an Olympus BX-61 microscope (Olympus America, Center Valley, PA) equipped with a Retiga 4000R color camera (QImaging, Surrey/BC, Canada).

Collagen Staining and Quantification and Immunofluorescent Staining

Three methods, Masson's Trichrome staining, Sirius red/fast green staining, and immunofluorescent staining against collagen III were used for collagen display.[49] The Masson trichrome stain kit was commercially available (IMEB, cat. #K7228), and the instructor's protocol was strictly followed. For Sirius red/fast green staining, the 8-μm-thin cryo-section tissues were fixed in prewarmed Bouin's solution for 20 min at 37°C followed by three times washing with tap water. Then, the slides were put in 0.2% (w/v) aqueous phosphomolybdic acid for 2 min, followed by washing prior to staining. The slides were stained in 0.1% fast green for 15–20 min, washed with tap water. Prior to Sirius red staining, the slides were dipped in 1% acetic acid for 2 min followed by washing with tap water. The slide was stained in 0.1% Sirius red for 15–20 min, washing with water. Next, the slides were dehydrated in 100% ethanol for three times, cleared in xylene, and mounted to the slides with permount. Sirius red was dissolved in saturated picric acid, and fast green was dissolved in distilled water. To quantify the collagen, the stained slides were eluted with dye extraction solution (a 1:1 mixture of 0.1 N NaOH and methanol), and the color was read at OD540 and OD605 by spectrophotometer. The collagen (μg/section) = (OD540 − [OD605 × 0.291])/37.8 × 1,000. Non-collagen protein (μg/section) = OD605 values/2.04 × 1,000. The goat anti-Type III Collagen-UNLB (cat. no. 1330-01, Southern Biotech Associates, Birmingham, AL) was used at 1:200, and the secondary antibody anti-goat CY3 (cat. no. C2821, Sigma-Aldrich, St. Louis, MO) was applied at 1:500. For mini-agrin staining, anti-rat-agrin antibody (cat. no. AF550, R&D Systems, Minneapolis, MN) was used at 1:100 on 9-μm thickness of cryo-sections.

Statistical Analysis

Values are expressed as means ± SEM. Welch's t test was applied when comparing two groups. When comparing three groups, one-way ANOVA plus Dunnett post-test was applied using Graph Pad Prism software. $p < 0.05$ was considered statistically significant. For the experiments involving multiple groups at different time points, two-way ANOVAs plus Bonferroni post-tests were used for statistical analysis. The mouse experiments were not done in a blinded fashion.

SUPPLEMENTAL INFORMATION

Supplemental Information includes eight figures, one table, and two movies and can be found with this article online at https://doi.org/10.1016/j.omtm.2018.01.005.

AUTHOR CONTRIBUTIONS

C.Q., S.S.M., and X.X. were actively involved in conceptualization, methodology development, and writing of this manuscript. Q.J. was responsible for the critical editing of the manuscript. C.Q., Y.D., B.X., and V.D.N. directly performed animal experiments. Jianbin Li and Juan Li were involved in AAV vector production and titration for this study.

ACKNOWLEDGMENTS

The UNC Mouse Behavior Core is supported by grant U54HD079124 from NICHD. This work was supported by NIH/NINDS 1RO1 NS079568 to X.X. Transmission electron microscopy and toluidine blue staining were performed at the UNC Microscopy Service Laboratory.

REFERENCES

1. Allamand, V., and Guicheney, P. (2002). Merosin-deficient congenital muscular dystrophy, autosomal recessive (MDC1A, MIM#156225, LAMA2 gene coding for alpha2 chain of laminin). Eur. J. Hum. Genet. *10*, 91–94.
2. Pegoraro, E., Fanin, M., Trevisan, C.P., Angelini, C., and Hoffman, E.P. (2000). A novel laminin alpha2 isoform in severe laminin alpha2 deficient congenital muscular dystrophy. Neurology *55*, 1128–1134.
3. O'Brien, D.P., Johnson, G.C., Liu, L.A., Guo, L.T., Engvall, E., Powell, H.C., and Shelton, G.D. (2001). Laminin alpha 2 (merosin)-deficient muscular dystrophy and demyelinating neuropathy in two cats. J. Neurol. Sci. *189*, 37–43.
4. Kuang, W., Xu, H., Vachon, P.H., Liu, L., Loechel, F., Wewer, U.M., and Engvall, E. (1998). Merosin-deficient congenital muscular dystrophy. Partial genetic correction in two mouse models. J. Clin. Invest. *102*, 844–852.
5. Geranmayeh, F., Clement, E., Feng, L.H., Sewry, C., Pagan, J., Mein, R., Abbs, S., Brueton, L., Childs, A.M., Jungbluth, H., et al. (2010). Genotype-phenotype correlation in a large population of muscular dystrophy patients with LAMA2 mutations. Neuromuscul. Disord. *20*, 241–250.
6. Valencia, C.A., Ankala, A., Rhodenizer, D., Bhide, S., Littlejohn, M.R., Keong, L.M., Rutkowski, A., Sparks, S., Bonnemann, C., and Hegde, M. (2013). Comprehensive mutation analysis for congenital muscular dystrophy: a clinical PCR-based enrichment and next-generation sequencing panel. PLoS ONE *8*, e53083.
7. Ding, J., Zhao, D., Du, R., Zhang, Y., Yang, H., Liu, J., Yan, C., Zhang, F., and Xiong, H. (2016). Clinical and molecular genetic analysis of a family with late-onset LAMA2-related muscular dystrophy. Brain Dev. *38*, 242–249.
8. Chan, S.H., Foley, A.R., Phadke, R., Mathew, A.A., Pitt, M., Sewry, C., and Muntoni, F. (2014). Limb girdle muscular dystrophy due to LAMA2 mutations: diagnostic difficulties due to associated peripheral neuropathy. Neuromuscul. Disord. *24*, 677–683.
9. Bönnemann, C.G., Wang, C.H., Quijano-Roy, S., Deconinck, N., Bertini, E., Ferreiro, A., Muntoni, F., Sewry, C., Béroud, C., Mathews, K.D., et al.; Members of International Standard of Care Committee for Congenital Muscular Dystrophies (2014). Diagnostic approach to the congenital muscular dystrophies. Neuromuscul. Disord. *24*, 289–311.
10. Wang, C.H., Bonnemann, C.G., Rutkowski, A., Sejersen, T., Bellini, J., Battista, V., Florence, J.M., Schara, U., Schuler, P.M., Wahbi, K., et al.; International Standard of Care Committee for Congenital Muscular Dystrophy (2010). Consensus statement on standard of care for congenital muscular dystrophies. J. Child Neurol. *25*, 1559–1581.
11. Kang, P.B., Morrison, L., Iannaccone, S.T., Graham, R.J., Bönnemann, C.G., Rutkowski, A., Hornyak, J., Wang, C.H., North, K., Oskoui, M., et al.; Guideline Development Subcommittee of the American Academy of Neurology and the Practice Issues Review Panel of the American Association of Neuromuscular & Electrodiagnostic Medicine (2015). Evidence-based guideline summary: evaluation, diagnosis, and management of congenital muscular dystrophy: report of the guideline development subcommittee of the american academy of neurology and the practice issues review panel of the american association of neuromuscular & electrodiagnostic medicine. Neurology *84*, 1369–1378.
12. Haliloglu, G., and Topaloglu, H. (2015). Evidence-based guideline summary: Evaluation, diagnosis, and management of congenital muscular dystrophy: report of the guideline development subcommittee of the american academy of neurology and the practice issues review panel of the american association of neuromuscular & electrodiagnostic medicine. Neurology *85*, 1432–1433.
13. Ervasti, J.M., and Campbell, K.P. (1991). Membrane organization of the dystrophin-glycoprotein complex. Cell *66*, 1121–1131.
14. Hall, T.E., Bryson-Richardson, R.J., Berger, S., Jacoby, A.S., Cole, N.J., Hollway, G.E., Berger, J., and Currie, P.D. (2007). The zebrafish candyfloss mutant implicates extracellular matrix adhesion failure in laminin alpha2-deficient congenital muscular dystrophy. Proc. Natl. Acad. Sci. USA *104*, 7092–7097.
15. Gawlik, K.I., and Durbeej, M. (2011). Skeletal muscle laminin and MDC1A: pathogenesis and treatment strategies. Skelet. Muscle *1*, 9.
16. D'Alessandro, M., Naom, I., Ferlini, A., Sewry, C., Dubowitz, V., and Muntoni, F. (1999). Is there selection in favour of heterozygotes in families with merosin-deficient congenital muscular dystrophy? Hum. Genet. *105*, 308–313.
17. Emery, A.E. (2002). The muscular dystrophies. Lancet *359*, 687–695.
18. Moll, J., Barzaghi, P., Lin, S., Bezakova, G., Lochmüller, H., Engvall, E., Müller, U., and Ruegg, M.A. (2001). An agrin minigene rescues dystrophic symptoms in a mouse model for congenital muscular dystrophy. Nature *413*, 302–307.
19. Bentzinger, C.F., Barzaghi, P., Lin, S., and Ruegg, M.A. (2005). Overexpression of mini-agrin in skeletal muscle increases muscle integrity and regenerative capacity in laminin-alpha2-deficient mice. FASEB J. *19*, 934–942.
20. Gawlik, K., Miyagoe-Suzuki, Y., Ekblom, P., Takeda, S., and Durbeej, M. (2004). Laminin alpha1 chain reduces muscular dystrophy in laminin alpha2 chain deficient mice. Hum. Mol. Genet. *13*, 1775–1784.
21. McKee, K.K., Crosson, S.C., Meinen, S., Reinhard, J.R., Rüegg, M.A., and Yurchenco, P.D. (2017). Chimeric protein repair of laminin polymerization ameliorates muscular dystrophy phenotype. J. Clin. Invest. *127*, 1075–1089.
22. Reinhard, J.R., Lin, S., McKee, K.K., Meinen, S., Crosson, S.C., Sury, M., Hobbs, S., Maier, G., Yurchenco, P.D., and Rüegg, M.A. (2017). Linker proteins restore basement membrane and correct LAMA2-related muscular dystrophy in mice. Sci. Transl. Med. *9*, eaal4649.
23. Girgenrath, M., Dominov, J.A., Kostek, C.A., and Miller, J.B. (2004). Inhibition of apoptosis improves outcome in a model of congenital muscular dystrophy. J. Clin. Invest. *114*, 1635–1639.
24. Dominov, J.A., Kravetz, A.J., Ardelt, M., Kostek, C.A., Beermann, M.L., and Miller, J.B. (2005). Muscle-specific BCL2 expression ameliorates muscle disease in laminin {alpha}2-deficient, but not dystrophin-deficient, mice. Hum Mol Genet *14*, 1029–1040.
25. Girgenrath, M., Beermann, M.L., Vishnudas, V.K., Homma, S., and Miller, J.B. (2009). Pathology is alleviated by doxycycline in a laminin-alpha2-null model of congenital muscular dystrophy. Ann. Neurol. *65*, 47–56.
26. Dunbar, C.E., and Emmons, R.V. (1994). Gene transfer into hematopoietic progenitor and stem cells: progress and problems. Stem Cells *12*, 563–576.
27. Carmignac, V., Quéré, R., and Durbeej, M. (2011). Proteasome inhibition improves the muscle of laminin α2 chain-deficient mice. Hum. Mol. Genet. *20*, 541–552.
28. Meinen, S., Lin, S., and Ruegg, M.A. (2012). Angiotensin II type 1 receptor antagonists alleviate muscle pathology in the mouse model for laminin-α2-deficient congenital muscular dystrophy (MDC1A). Skelet. Muscle *2*, 18.
29. Erb, M., Meinen, S., Barzaghi, P., Sumanovski, L.T., Courdier-Früh, I., Rüegg, M.A., and Meier, T. (2009). Omigapil ameliorates the pathology of muscle dystrophy caused by laminin-alpha2 deficiency. J. Pharmacol. Exp. Ther. *331*, 787–795.
30. Meinen, S., and Ruegg, M.A. (2006). Congenital muscular dystrophy: mini-agrin delivers in mice. Gene Ther. *13*, 869–870.
31. Qiao, C., Li, J., Zhu, T., Draviam, R., Watkins, S., Ye, X., Chen, C., Li, J., and Xiao, X. (2005). Amelioration of laminin-alpha2-deficient congenital muscular dystrophy by somatic gene transfer of miniagrin. Proc. Natl. Acad. Sci. USA *102*, 11999–12004.
32. Xiao, W., Chirmule, N., Berta, S.C., McCullough, B., Gao, G., and Wilson, J.M. (1999). Gene therapy vectors based on adeno-associated virus type 1. J. Virol. *73*, 3994–4003.
33. Gao, G.P., Alvira, M.R., Wang, L., Calcedo, R., Johnston, J., and Wilson, J.M. (2002). Novel adeno-associated viruses from rhesus monkeys as vectors for human gene therapy. Proc. Natl. Acad. Sci. USA *99*, 11854–11859.
34. Inagaki, K., Fuess, S., Storm, T.A., Gibson, G.A., Mctiernan, C.F., Kay, M.A., and Nakai, H. (2006). Robust systemic transduction with AAV9 vectors in mice: efficient global cardiac gene transfer superior to that of AAV8. Mol. Ther. *14*, 45–53.
35. Huang, H.S., Burns, A.J., Nonneman, R.J., Baker, L.K., Riddick, N.V., Nikolova, V.D., Riday, T.T., Yashiro, K., Philpot, B.D., and Moy, S.S. (2013). Behavioral deficits in an Angelman syndrome model: effects of genetic background and age. Behav. Brain Res. *243*, 79–90.

36. Di Scipio, F., Raimondo, S., Tos, P., and Geuna, S. (2008). A simple protocol for paraffin-embedded myelin sheath staining with osmium tetroxide for light microscope observation. Microsc. Res. Tech. *71*, 497–502.

37. Yurchenco, P.D. (2011). Basement membranes: cell scaffoldings and signaling platforms. Cold Spring Harb. Perspect. Biol. *3*, a004911.

38. Arroyo, E.J., Bermingham, J.R., Jr., Rosenfeld, M.G., and Scherer, S.S. (1998). Promyelinating Schwann cells express Tst-1/SCIP/Oct-6. J. Neurosci. *18*, 7891–7902.

39. Häger, M., Gawlik, K., Nyström, A., Sasaki, T., and Durbeej, M. (2005). Laminin alpha1 chain corrects male infertility caused by absence of laminin alpha2 chain. Am. J. Pathol. *167*, 823–833.

40. Gimeno, H., Gordon, A., Tustin, K., and Lin, J.P. (2013). Functional priorities in daily life for children and young people with dystonic movement disorders and their families. Eur. J. Paediatr. Neurol. *17*, 161–168.

41. Wang, B., Li, J., Fu, F.H., Chen, C., Zhu, X., Zhou, L., Jiang, X., and Xiao, X. (2008). Construction and analysis of compact muscle-specific promoters for AAV vectors. Gene Ther. *15*, 1489–1499.

42. Guo, L.T., Zhang, X.U., Kuang, W., Xu, H., Liu, L.A., Vilquin, J.T., Miyagoe-Suzuki, Y., Takeda, S., Ruegg, M.A., Wewer, U.M., and Engvall, E. (2003). Laminin alpha2 deficiency and muscular dystrophy; genotype-phenotype correlation in mutant mice. Neuromuscul. Disord. *13*, 207–215.

43. Homma, S., Beermann, M.L., and Miller, J.B. (2011). Peripheral nerve pathology, including aberrant Schwann cell differentiation, is ameliorated by doxycycline in a laminin-α2-deficient mouse model of congenital muscular dystrophy. Hum. Mol. Genet. *20*, 2662–2672.

44. Gawlik, K.I., Li, J.Y., Petersén, A., and Durbeej, M. (2006). Laminin alpha1 chain improves laminin alpha2 chain deficient peripheral neuropathy. Hum. Mol. Genet. *15*, 2690–2700.

45. Bassat, E., Mutlak, Y.E., Genzelinakh, A., Shadrin, I.Y., Baruch Umansky, K., Yifa, O., Kain, D., Rajchman, D., Leach, J., Riabov Bassat, D., et al. (2017). The extracellular matrix protein agrin promotes heart regeneration in mice. Nature *547*, 179–184.

46. Qiao, C., Yuan, Z., Li, J., He, B., Zheng, H., Mayer, C., Li, J., and Xiao, X. (2011). Liver-specific microRNA-122 target sequences incorporated in AAV vectors efficiently inhibits transgene expression in the liver. Gene Ther. *18*, 403–410.

47. Ayuso, E., Mingozzi, F., Montane, J., Leon, X., Anguela, X.M., Haurigot, V., Edmonson, S.A., Africa, L., Zhou, S., High, K.A., et al. (2010). High AAV vector purity results in serotype- and tissue-independent enhancement of transduction efficiency. Gene Ther. *17*, 503–510.

48. Reynolds, E.S. (1963). The use of lead citrate at high pH as an electron-opaque stain in electron microscopy. J. Cell Biol. *17*, 208–212.

49. Qiao, C., Wang, C.H., Zhao, C., Lu, P., Awano, H., Xiao, B., Li, J., Yuan, Z., Dai, Y., Martin, C.B., et al. (2014). Muscle and heart function restoration in a limb girdle muscular dystrophy 2I (LGMD2I) mouse model by systemic FKRP gene delivery. Mol Ther. *22*, 1890–1899.